# The magnetic ordering in high magnetoresistance Mn-doped ZnO thin films

Cite as: AIP Advances **6**, 035019 (2016); https://doi.org/10.1063/1.4944954
Submitted: 11 November 2015 • Accepted: 17 March 2016 • Published Online: 24 March 2016

**S. Venkatesh, A. Baras, J.-S. Lee, et al.**

# The magnetic ordering in high magnetoresistance Mn-doped ZnO thin films

S. Venkatesh,[1] A. Baras,[1] J.-S. Lee,[2] and I. S. Roqan[1,a]
[1]*Physical Sciences and Engineering Division, King Abdullah University of Science and Technology (KAUST), Thuwal 23955-6900, Saudi Arabia*
[2]*Stanford Synchrotron Radiation Lightsource, SLAC National Accelerator Laboratory, Menlo Park, California 94025, USA*

(Received 11 November 2015; accepted 17 March 2016; published online 24 March 2016)

We studied the nature of magnetic ordering in Mn-doped ZnO thin films that exhibited ferromagnetism at 300 K and superparamagnetism at 5 K. We directly interrelated the magnetisation and magnetoresistance by invoking the polaron percolation theory and variable range of hopping conduction below the metal-to-insulator transition. By obtaining a qualitative agreement between these two models, we attribute the ferromagnetism to the *s-d* exchange-induced spin splitting that was indicated by large positive magnetoresistance (~40 %). Low temperature superparamagnetism was attributed to the localization of carriers and non-interacting polaron clusters. This analysis can assist in understanding the presence or absence of ferromagnetism in doped/un-doped ZnO.  [http://dx.doi.org/10.1063/1.4944954]

## I. INTRODUCTION

The emerging field of spintronics based on diluted magnetic semiconductors (DMS) requires intrinsic room temperature ferromagnetism (RTFM) in a semiconductor.[1] ZnO, a wide band-gap semiconductor, was proposed as a potential candidate upon doping with Mn.[2] Among the *3d* transition metals (TM), solubility of $Mn^{2+}$ ($3d^5$) in ZnO is believed to be high (~35 %).[3] Furthermore, metallic nanocrystals embedded in oxides have been attracting considerable interest due to the potential for their use in spintronic devices.[4,5] Recently, transition metal (TM) segregation in ZnO thin film was found to result in high magnetoresistance, which can act as spin filters for the electrons, promising new generation of spintronic applications.[6] However, conflicting or irreproducible magnetisation results were often reported.[7–9] For instance, high level doping of Mn in ZnO led to clusters and consequently distance-dependent Mn-Mn interactions favored antiferromagnetic state.[10] In some cases, ferromagnetism at room temperature and superparamagnetism (SPM) at low temperature were observed.[11–14] Although such observations of coexistence of two different magnetic states in doped or even in un-doped ZnO[13] has been reported,[11–14] the origin of this phenomenon remains unclear. Therefore, it is important to investigate the nature and origin of magnetic ordering, in doped ZnO beyond achieving RTFM.

In the present study, we aim to broaden our understanding of the coexistence of SPM and RTFM in the Mn-doped ZnO thin films by invoking the carrier localization effect that is manifested in the magnetic and magneto-transport properties. The objective of this work is to explore the origin of SPM that emerge at low temperatures in the Mn-doped ZnO thin films. Similar LT-SPM behavior studied by Sawicki *et al*. in Mn-doped GaAs[15] and Chao *et al*. in Co-doped ZnO[16] was attributed to the interplay between ferromagnetism and carrier localization. We apply the polaron percolation model and Mott's variable range of hopping near the metal-to-insulator transition (MIT) to analyze the origin of the SPM. We directly inter-relate the magnetic and magnetoresistance properties and

[a]Corresponding author: Iman.roqan@kaust.edu.sa

 

observe qualitative agreement between the bound magnetic polarons (BMP) formalism and Mott's variable range of hopping (VRH) conduction to account for the low temperature superparamagnetism (LT-SPM).

## II. EXPERIMENT

Several Mn-doped ZnO thin films were deposited by pulsed laser deposition (PLD) on various types of substrates (*c*-, *a*-plane sapphire, LSAT and Si) using a KrF laser ($\lambda$ = 248 nm) with a substrate temperature of 600 °C. Mn 2at%-doped ZnO PLD target was prepared using highly pure oxide powders (ZnO 99.999 % and MnO 99.99 %, both from Sigma Aldrich) by ball milling the powders weighed to the stoichiometry and pressing it into a dense pellet of 1-inch diameter that was subsequently sintered in air at 1050 °C for 12 hours. As it is well known that ZnO thin films deposited under oxygen-rich and -poor conditions lead to various types of defects and related magnetic and transport properties,[17] we varied the oxygen partial pressure ($P(O_2)$) during the deposition. As the magnetic behaviors of all thin films were similar, we chose two representative thin films that were deposited in the extreme $P(O_2)$-controllable range of 50 and 500 mTorr in our PLD chamber (Neocerra, USA). We labelled these films as sample A and sample B that were grown on *c*-sapphire, respectively, unless otherwise specified. X-ray diffraction (XRD) patterns were collected by utilizing a Bruker D8-Discover. Microstructure analyses were carried out using Helios 400S-FEI high-resolution scanning electron microscope (SEM), and Titan-FEI transmission electron microscope (TEM). Elemental quantification was performed by wavelength dispersive X-ray spectroscopy (WDS). X-ray photoelectron spectroscopy (XPS) experiments were carried out by employing Al-K$\alpha$ (h$\nu$ = 1486.6 eV) X-ray source operated at 150 W in a Kratos Axis Ultra DLD. Magnetisation measurements were carried out in a SQUID vibrating sample magnetometer (SVSM, Quantum design) in the temperature (T) range of 5 K to 300 K and in the magnetic field (H) range of ±5 T. All the measurements were obtained with the field applied parallel to the plane of the thin films. Care was taken to exclude the response of the substrate and the discrepancies in the SQUID magnetometry,[18] thus allowing us to extract the magnetisation data pertaining solely to the thin films. We studied the Hall-effect and resistivity as a function of magnetic field and temperature in a physical property measurement system (PPMS, Quantum design). Near-edge X-ray absorption spectroscopy (XAS) was conducted in BL 8-2, at the Stanford Synchrotron Radiation Lightsource (SSRL).

## III. RESULTS AND DISCUSSION

The XRD patterns of thin films A and B (Fig. 1) show peaks corresponding only to the (0 0 l) planes, indicating equiaxial growth of the Mn-doped ZnO thin films along the *c*-axis of the ZnO wurtzite structure. A typical SEM micrograph shows the nanograins from the top view and the cross-sectional columnar growth of the thin films (as shown in Figs. 2(a) and 2(b), respectively).

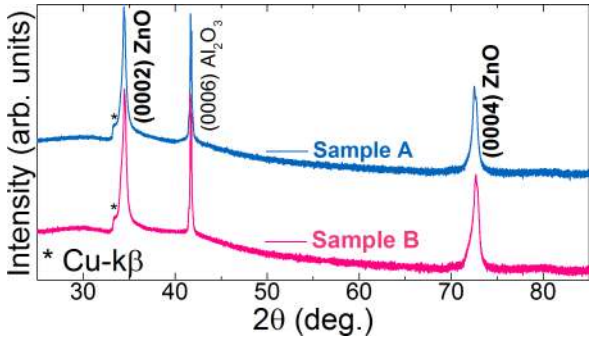


FIG. 1. XRD patterns (2θ-θ scan) of Mn-doped ZnO thin films grown on *c*-sapphire.

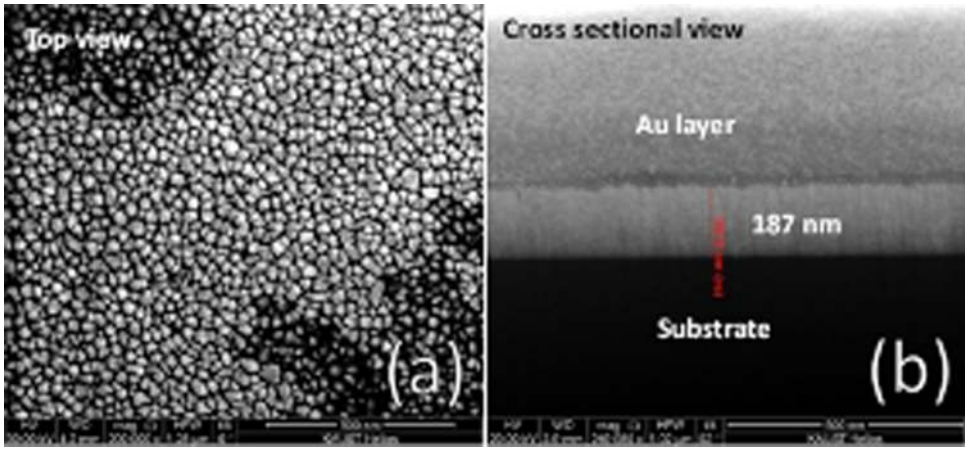


FIG. 2. SEM micrographs of sample A deposited at 50 mTorr showing (a) top and (b) cross-sectional views of highly oriented nanograins and columnar growth of the thin films.

Wavelength dispersive X-ray spectroscopy (WDS) analyses (data not shown) revealed that the concentration of Mn in these films were just below 2 at%. The thickness of these samples were estimated by cross sectional SEM (Fig. 2(b)) and is found to be 187 nm for sample A and 247 nm for sample B.

Typical HRTEM micrographs (Fig. 3(a) and 3(b)) and the fast Fourier transform (FFT) diffraction patterns (inset of Fig. 3(b)) confirm the [002] orientation of the films. However, the contrast in the cross section of the HRTEM image (Fig. 3(a)) shows inhomogeneous feature may imply inclusion of Mn nanoclusters or secondary phases. In order to ascertain the chemical state of the elements, XPS and XAS experiments were carried out on these samples.

Fig. 4(a) shows the XPS spectra of the Mn-doped ZnO thin films. As can be seen in the full scan spectra, the peaks corresponding to Zn, O, Mn and adventitious C are visible. The chemical state of the Zn atoms was analyzed by examining the Auger $ZnL_3M_{4,5}M_{4,5}$ peaks. It is thus suggestive that Zn remains in $Zn^{2+}$ state. Photoelectron peaks corresponding to the Mn-*2p* and Mn-*3p* are observed near 640.73 eV and 48 eV, respectively, suggesting that Mn also remains in the $Mn^{2+}$ state.[19] Therefore, the existence of MnO secondary phases in Mn-doped ZnO is expected in this material. Fig. 4(b) shows the near-edge XAS spectra collected at the O$K-$ edge from the

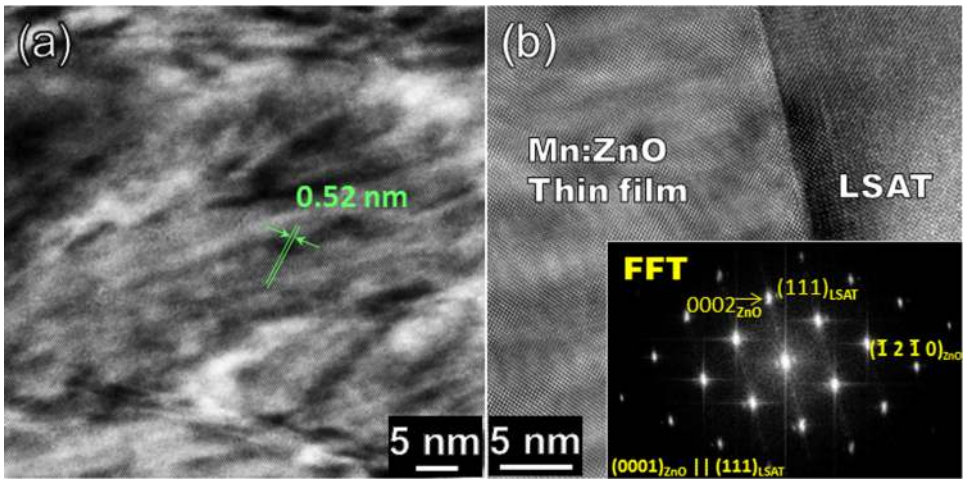


FIG. 3. HRTEM micrographs of sample A showing (a) (002) planes (b) thin films–substrate interface and the inset shows diffraction patterns along the $[11\text{-}20]_{ZnO}$ zone axis; additional spots are from the LSAT substrate showing the $(0001)_{ZnO}//(111)_{LSAT}$ epitaxial relationship.

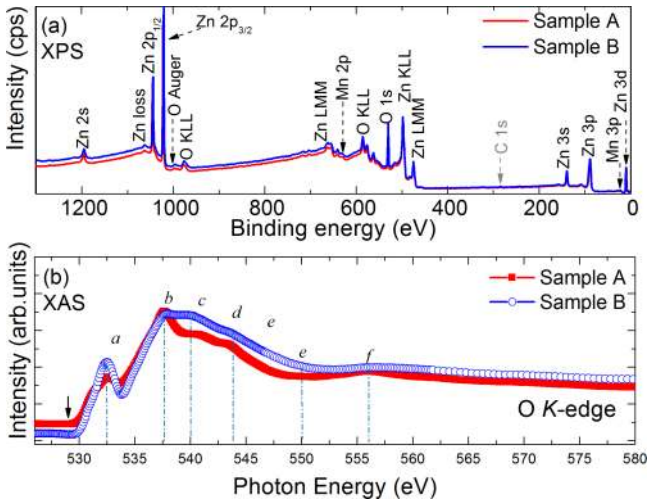


FIG. 4. (a) XPS spectra and (b) near edge XAS spectra from sample A (50 mTorr) and sample B (500 mTorr).

two Mn-doped ZnO films. No pre-edge feature located at 529 eV (pointed by arrow in Fig. 4(b)) is observed; this peak can be observed for highly impurity doped ZnO samples only (>2%) and increases as Mn concentration increases.[20–22] The pre-edge feature was referred to dipole transitions from O 1s to O *2p* states that is hybridized with the unoccupied Mn *3d* states. Therefore, the intensity of this peak represents the Mn *3d* density of states. Thus, the disappearance of this peak occurs at low Mn concentration, indicating, less unoccupied states at the Mn *3d* levels, leading to lower carrier concentration (electrons) compared to highly doped (>2%).[23] Therefore, the absence of such feature suggests that the Mn doping level is low in these two films. Our observation is consistent with a previous study (2.2 at%) Mn-doped ZnO.[24] We denoted various peak positions in the XAS spectra by labelling them with letters (*a*-*f*). Peak *a* can be attributed to the hybridization of O-*2p* with highly dispersive cation states (Zn *3d4s*/Mn*3d*) forming the bottom of the conduction band that peaks at ~541 eV (peak *b*) due to the transition to O $2p_z$ and $2p_{x+y}$ states.[25] Peaks *c* to *f* are attributed to the hybridization of O-*2p* with the cation core states (Zn-*4p* and Mn-*4sp*).[20,26] The intensity of peak *a* is suggestive of the strength of the *p*-*d* hybridization induced by Mn doping. Therefore, the Mn bonds are stronger in sample B than that in sample A. Since the spectral features are sensitive to the angle of incidence and any asymmetry of the $\sigma$-bonds (normal to the *c*-axis) and $\pi$-bonds (parallel to the *c*-axis),[27] any difference in the orientation of the nanostructured grains with respect to the incident x-ray beam could also affect the spectral intensities between the two samples.

Fig. 5(a) and 5(b) show the magnetisation hysteresis loops at 5 K and 300 K, while the insets of the bottom right panels of Fig. 5(a) and 5(b) depict the magnified central portions of the loops. The opening of the MH loops is clearly visible near the origin. For measuring the temperature variation of magnetisation, each sample was initially cooled from the room temperature to 5 K without applying any field. A field of H = 1000 Oe was subsequently applied and the data were recorded while warming (ZFC) to 350 K. The same process was repeated while cooling from 350K to 5 K under the same applied field (FC). The ZFC-FC curves shown in Fig. 5(c) and 5(d) indicate that neither of the samples showed any Curie transition for the temperature range used in this work. It can be observed in Fig. 5 that MH loops of both samples are ferromagnetic at room temperature. The saturation magnetisation (MS) decreases from 3.22 emu/cc for sample A to 1.33 emu/cc for sample B. Earlier reports suggested that FM observed either in un-doped or Mn-doped ZnO nanograined thin films is strongly dependent on the ratio ($R_G$) of the grain boundary area (GBA) to the grain volume (GV), which must exceed certain threshold value.[28,29] According to the results of the SEM analyses (Fig. 2(a)), these thin films have closely arranged equiaxial nanograins. The mean area of the nanograins in the present case is >300 $nm^2$ and the value of $R_G > 5 \times 10^8$ $m^{-1}$. This value is few orders higher than the threshold value of $R_G(2 \pm 4 \times 10^5$ $m^{-1})$ required for FM in Mn-doped ZnO[28] thin films. For instance, only paramagnetic state was observed in un-doped ZnO thin films

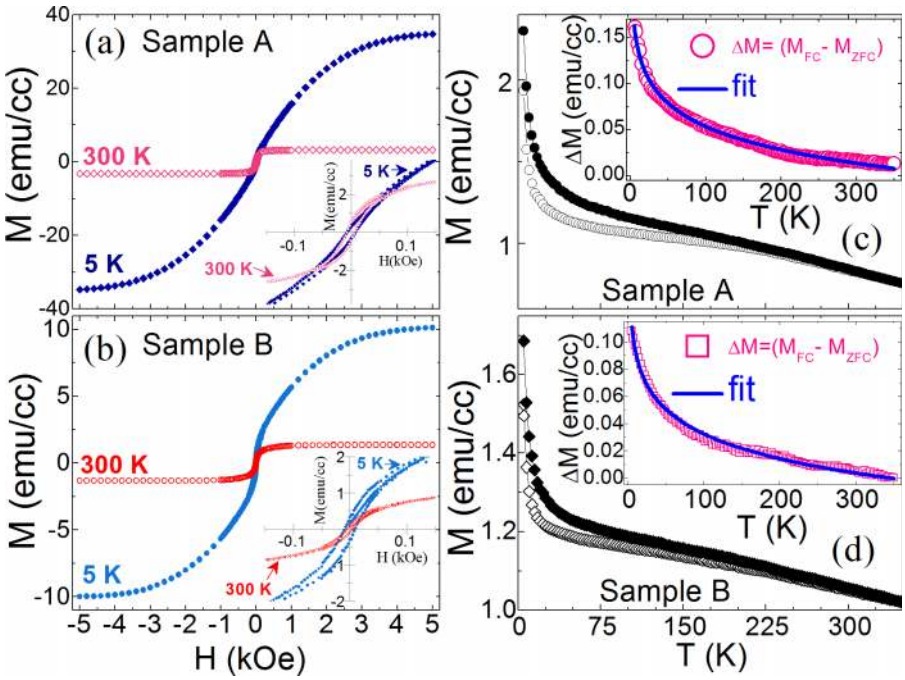


FIG. 5. MH loops (a, b) and ZFC-FC magnetisation (c, d) of samples A and B, respectively. The insets of panels (c) and (d) show the Kaminski-Das Sarma fit of the polaron percolation model.

when $2 \pm 4 \times 10^5$ m$^{-1}$ < $R_G$ < $5 \pm 3 \times 10^7$ m$^{-1}$,[28] suggesting that the grain boundaries and related vacancies play a major role in determining the magnetic properties. It is also worth noting that point defects and impurity segregation present at the grain boundaries of oxides could trap electrons and form polarons.[30] Stochastic distribution of such point defects would give rise to SPM[31] due to the formation of BMPs.

Fig. 5(a) and 5(b) shows that the MH loops of both samples at 5 K, are unsaturated even at 5 Tesla and exhibit a SPM-like response. The estimated low temperature magnetic moment (~7 $\mu_B$/Mn, by considering the actual Mn concentration of 1.3 at% and the density of pure ZnO = 5.606 g/cm$^3$) is unexpectedly high and above the high spin state of Mn and is, therefore, not arising from Mn; it can be rather due to defects related to vacancies[32] or strains.[13] The LT-SPM-like behavior could be due to the competing effects of FM and SPM in the system.[33] Such an anomaly in magnetisation was also observed in Mn-doped GaAs in which an additional contribution that coexisted (at low temperature) with the spontaneous magnetisation was attributed to a nanoscale phase separation due to quantum critical fluctuations.[15] The quantum critical fluctuations influence the resulting magnetic ordering near the metal-to-insulator transitions that is, in turn, dependent on the localization of carriers. The temperature below which this LT-SPM-like behavior evolved was identified as relevant blocking temperature.[15]

We believe that a pseudo-superparamagnetic phase evolves at low temperatures (<50 K, in the present case) due to carrier localization.[15] Carrier localization that take place at structural defect sites, such as point defects, GB, Mn clusters or MnO or other secondary phases embedded in ZnO could form BMPs, and it has remarkable implications for the magnetic properties of DMS. According to the polaron percolation model for DMS,[34,35] localized carriers trapped at these defect sites could polarize the Mn impurity spins falling within an effective field of interaction, thereby creating a BMP. Therefore, the electrons can be trapped in the defect sites in the thin films. Since the distribution of these defects created during the preparation of thin films is random, clusters of BMPs are created. Stochastic distribution of BMP clusters could give rise to LT- SPM[31] due to temperature-dependent carrier localization.

Under equilibrium conditions, the densities of electron trapping defects and the BMPs remain unchanged.[16] The interaction between the spin of the localized carrier $S_l$, and that of the impurity

$s_i$ within a polaron is antiferromagnetic, although interactions between neighboring polarons lead to ferromagnetic ordering of impurity spins in order to minimize their energy. The Hamiltonian for such a system is given by

$$H = \sum_{l,i} J_{li} S_l S_i \tag{1}$$

where J is the exchange integral and i and l denote the impurity and localized electrons, respectively. As the temperature decreases, the size of the polarons increases due to overlapping with other polarons,[34] and thus creating polaron clusters of ferromagnetically aligned impurity spins.[35] As the temperature decreases, a greater number of spins are ordered within each polaron, causing the magnetisation to increase and can lead to the observed high magnetic moment (~7 $\mu_B$/Mn) at 5K. In a wide and direct bandgap semiconductor, the BMP is localized even at high temperatures, leading to a high magnetic moment at low temperature.[36,37] The spin of the magnetic impurities/defects involved in BMP will be polarized, and will couple to the spin of electrons. Therefore, each aligned trapped electron couples the local magnetic moment of the host atoms that lie within the BMP, resulting in a high magnetic moment. However, the BMPs are not connected throughout the sample because the defect centres (at which each BMP evolves) are inhomogeneously distributed, resulting in polaron clusters.[31,38] Since these clusters of BMPs are lacking in long range ordering, a LT-SPM-like magnetisation curve is exhibited at 5 K. At sufficiently high temperatures (300 K), polarons are not percolated because carriers are confined to a few sites; hence, the resulting magnetisation is saturated.[39] This mechanism is different from that of the high temperature SPM due to the spinodal decomposition.[40] The temperature dependence and shape of the magnetisation curve can be determined by the product of the carrier concentration and the radius of the polaron by applying the polaron percolation model proposed by Kaminski and Das Sarma.[34,35]

According to this model,[34,35] the expression for the temperature variation of magnetisation in strongly correlated polarons is given by

$$M(T) \propto 0.86 + (a_B^3 n_c)^{1/3} \ln\left(\frac{T_C}{T}\right) \tag{2}$$

where $a_B$ is the decaying wave function of the localized carrier, also known as the effective Bohr radius of the BMP, and $T_C$ is the Curie temperature. The $T_C$ value was assumed to be 300 K for the best fitting of Eqn. (2) for both samples, as we observed RTFM. Previous reports have also affirmed a lower value of $T_C$ from Eqn. (2) (see Ref. 23 in Ref. 34). Here, $n_c$ is the critical carrier concentration above which the carriers are delocalized and below which they are localized. In the present case, the carrier concentration $n_c > n_e$ is found, suggesting localization of carriers. The value of $n_e$ is $6.7 \times 10^{18}$ cm$^{-3}$ for sample A and $3.4 \times 10^{18}$ cm$^{-3}$ for sample B. It should be noted that the validity of this equation is limited by the condition of ($a_B^3 n_c << 1$). As a strong correlation between the BMPs was created at the defect sites, we obtained a good fit of the temperature variation of $\Delta M$ (=$M_{FC}$-$M_{ZFC}$) to Eqn. (2), as shown in the inset of Fig. 5(c) and 5(d) for sample A and B, respectively. The values of the derived parameter ($a_B^3 n_c$) were $1.43 \times 10^{-2}$ and $1.3 \times 10^{-3}$ for thin films A and B, respectively. Comparable values of $a_B^3 n_c$ were reported for Mn implanted in single-crystal Ge ($1.4 \times 10^{-2}$);[41] amorphous Ge (~$2.5 \times 10^{-3}$);[42] and $TiO_2$ ($1.68 \times 10^{-2}$);[43] while that related to Cr-doped amorphous Si was two orders of magnitude lower ($2.7 \times 10^{-5}$).[44] In all these cases, the value of $a_B^3 n_c$ was below unity, implying that the mean distance between localized electrons exceeded the electron's localization radius. This suggests the applicability of the percolation mechanism with localized carriers, pinned down within a polaron of radius $a_B$[34] to the present case. Thus, based on the experimental fit to Eqn. 2 and the value of ($a_B^3 n_c$), we confirm the percolation nature of the BMPs in our Mn-doped ZnO thin films. The SPM observed at 5 K is indeed an illustration of percolated, non-interacting clusters of polarons[31] formed at the inhomogeneously distributed clusters of electron trapping defects.[16]

We suggest that the percolation behavior of BMPs in these Mn-doped ZnO thin films follows a dynamic process that is strongly dependent on temperature and magnetic field. Therefore, the transport properties of these thin films should be affected by this process. Hence, the transport measurements were carried out using PPMS, by adapting the Van-der Pauw geometry. Fig. 6 shows

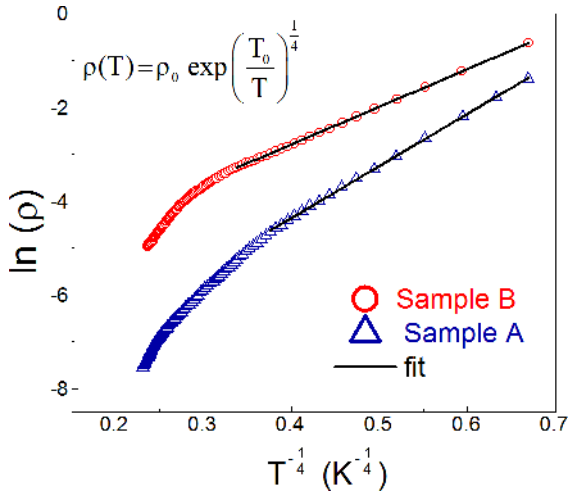


FIG. 6. 1/T1/4 dependence of ln(ρ) for sample A (triangles) and sample B (circles). The straight line represents the fit to Mott's VRH theory.

the linear $T^{-0.25}$ dependence on resistivity at low temperatures, suggesting VRH conduction in these thin films that is typically seen in ferromagnetic oxides with localized carriers.[16,45] According to this theory, the transport of charges takes place from one localized state to the next (energetically favorable) state, via hopping. Mott's VRH conduction from an occupied $m^{th}$ state to a vacant $n^{th}$ state for a three-dimensional case is given by

$$\rho(T) = \rho_0 \exp\left(\frac{T_0}{T}\right)^{1/4} \tag{3}$$

where $\rho_0$ is a temperature independent resistivity parameter and $T_0$ is a characteristic temperature. By fitting the experimental data shown in Fig. 6 to Eqn. (3), we observed that the conduction of both Mn-doped ZnO thin films at low temperature is governed by Mott's VRH mechanism.

The charge transport in the present case characterized by low $n_e$ (less than $n_c$) takes place via phonon-assisted quantum mechanical tunneling at low temperature.[46] This finding indicates that the carrier localization in these films is temperature dependent. At high temperatures (>170 K), a thermally activated $\rho(T) = \rho_0 \exp(\Delta E/K_B T)$-type conduction mechanism (fitting not shown) is dominant. For sample A and B, the thermal activation energy (ΔE) values were 58.7 meV and 33.7 meV, respectively, suggesting that the impurity band merges with the conduction band.[47] This observation is also in agreement with the magnetisation results. Sample B, which shows less localization depth than observed in sample A, exhibits lower magnetisation (this can be seen by comparing the scales in Fig. 5(a) and 5(b)) as highly localized carriers lead to isolated clusters of BMP spheres.[16]

We conducted magnetic field-dependent resistivity measurements at different temperatures to support our findings. The change in the magnetic field-dependent resistivity, termed as magnetoresistance (MR), is defined as $MR(\%) = [(R_H - R_{H=0})/R_{H=0}]^*100$. Manifestation of positive (increment) or negative (decrement) MR in a material is related to the carrier concentration and magnetic ordering.[48–50] The MR field dependence for sample A and B is shown in Fig. 7. A large positive MR of about 40 % is observed in both thin films at T ~10 K. However, the negative components admix with positive components below 10 K and at H above ±10 kOe. There is ~5 % reduction of MR at 5 K compared with 7.5 K at which the MR reaches its maximum and decreases thereafter. Above 7.5 K, the positive MR is dominant; however, it decreases monotonically as the temperature increases. Such variations of MR in Mn-doped ZnO thin films manifest the degree of carrier localization.[51] In this context, this phenomenon could be perceived as a transition from a pseudo-insulator to a metallic regime.

The large positive MR (~40 %) observed in these thin films suggests an *s-d* exchange-induced spin-splitting of the conduction band[52–54] and field-induced spin-flip scattering[50,55] of the disordered

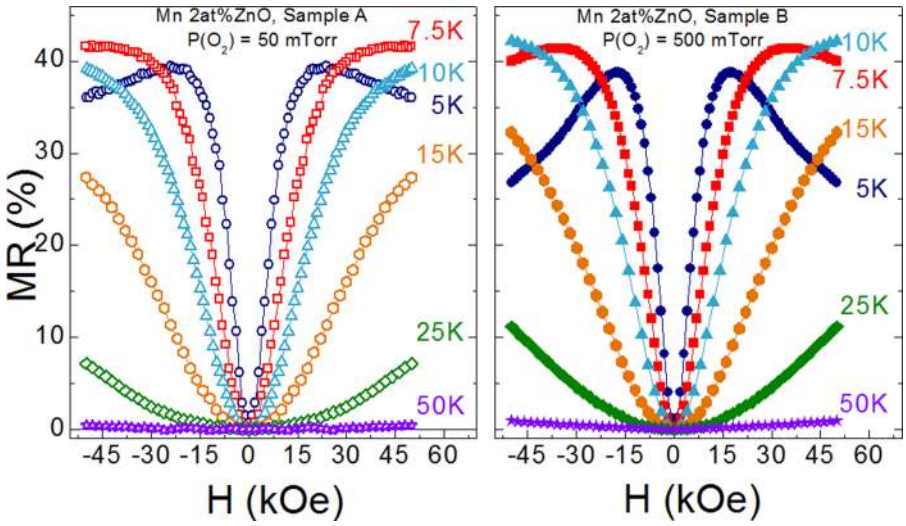


FIG. 7. Magnetoresistance of sample A (open symbols) and sample B (closed symbols).

spins to gain the majority spin direction is observed in the conduction band. The large positive MR and LT-SPM behavior can be due to the clustering of BMPs, while the negative MR is due to the formation of polarons.[55] At higher magnetic fields (H > 1 T), the strength of the field delocalize the electrons confined to the BMPs; consequently, the conduction increases, resulting in negative MR.[55]

The low-temperature MR and the magnetisation data suggest that co-existence of a ferromagnetic and a superparamagnetic phase is possible in these thin films, in the nearly insulator regime of a metal-to-insulator transition (MIT). The MIT depends both on temperature[46] and field. Therefore, we show the degree of carrier localization in the vicinity of MIT that can be determined by Mott's criterion:[46]

$$n_c^{1/3} a_B \leq 0.25 \tag{4}$$

The value of $n_c$ below which the carriers are localized is found by assuming $a_B$ (~0.76 nm) for pure ZnO,[56,57] and $(a_B n_c^{1/3}) \approx 0.25$ is $3.56 \times 10^{19}$ cm$^{-3}$. Indeed, in the present case, the electron concentrations at room temperature are well below this critical limit, affirming the localization of carriers at the defect sites and the formation of discrete polaron clusters. There is a good agreement near MIT for these thin films, while complying with the polaron percolation (Eqn. (2)) and VRH mechanism below $n_c$, *i.e.*, in a nearly insulating regime.[49,50]

## IV. CONCLUSIONS

We have observed a coexistence of FM and SPM in Mn-doped ZnO thin films, at low temperatures. XPS studies suggested substitution of $Mn^{2+}$ for $Zn^{2+}$ and therefore the formation of oxides of Mn cannot be excluded. Carrier localization at defects, clusters and secondary phases can lead to inhomogeneously distributed clusters of polarons, due to percolation; give rise to LT-SPM-like magnetisation at 5 K. This is demonstrated by obtaining a clear agreement between the percolation model and VRH conduction near MIT in the $Mn^{2+-}$ doped ZnO thin films. The field-induced delocalization contributes a negative component of MR below 10 K. Coexistence of SPM and FM phases at low temperature is due to the interplay between localization and the *s-d* exchange interaction of impurity spins, which led to large positive MR at 5 K.

## ACKNOWLEDGMENTS

The authors wish to thank KAUST for the financial support. Synchrotron studies were carried out at the SSRL, a Directorate of SLAC and an Office of Science User Facility operated for the

US DOE Office of Science by Stanford University. J.S.L. acknowledges partial funding from the Global Research Laboratory program of the Korean Ministry of Education, Science, and Technology (MEST). The authors also thank Dr. Paul R Edwards and Prof. Robert W Martin for using EPMA facilities at University of Strathclyde.

[1] S. A. Wolf, D. D. Awschalom, R. A. Buhrman, J. M. Daughton, S. von Molnar, M. L. Roukes, A. Y. Chtchelkanova, and D. M. Treger, Science **294**, 1488 (2001).
[2] T. Dietl, Science **287**, 1019 (2000).
[3] T. Fukumura, Z. Jin, M. Kawasaki, T. Shono, T. Hasegawa, S. Koshihara, and H. Koinuma, Appl. Phys. Lett. **78**(7), 958 (2001).
[4] N. Jedrecy, H. J. von Bardeleben, and D. Demaille, Phys. Rev. B **80**, 205204 (2009).
[5] D. Y. Li, Y. J. Zeng, L. M. C. Pereira, D. Batuk, J. Hadermann, Y. Z. Zhang, Z. Z. Ye, K. Temst, A. Vantomme, M. J. Van Bael, and C. Van Haesendonck, J. App. Phys. **114**(3), 033909 (2013).
[6] M. Hamieh, N. Jedrecy, C. Hebert, D. Demaille, and J. Perriere, Phys. Rev. B **92**, 155302 (2015).
[7] J. Alaria, P. Turek, M. Bernard, M. Bouloudenine, A. Berbadj, N. Brihi, G. Schmerber, S. Colis, and A. Dinia, Chem. Phys. Lett. **415**(4-6), 337 (2005).
[8] C. N. R. Rao and F. L. Deepak, J. Mater. Chem. **15**(5), 573 (2005).
[9] S. W. Jung, S.-J. An, G.-C. Yi, C. U. Jung, and S.-I. Lee, Appl. Phys. Lett. **80**(24), 4561 (2002).
[10] P. Sharma, A. Gupta, K. V. Rao, F. J. Owens, R. Sharma, R. Ahuja, J. M. Guillen, B. Johansson, and G. A. Gehring, Nature Mater. **2**(10), 673 (2003).
[11] D. A. Schwartz and D. R. Gamelin, Adv. Mater. **16**(23-24), 2115 (2004).
[12] F. Zhu, Y. Zhang, Y. Yan, W. Song, and L. Xia, Bull. Mater. Sci. **31**(2), 121 (2008).
[13] F. Schoofs, T. Fix, A. Hakimi, S. S. Dhesi, G. van der Laan, S. A. Cavill, S. Langridge, J. L. MacManus-Driscoll, and M. G. Blamire, J. Appl. Phys. **108**(5), 053911 (2010).
[14] N. S. Norberg, K. R. Kittilstved, J. E. Amonette, R. K. Kukkadapu, D. A. Schwartz, and a. D. R. Gamelin, J. Am. Chem. Soc **126**(30), 9387 (2004).
[15] M. Sawicki, D. Chiba, A. Korbecka, Y. Nishitani, J. A. Majewski, F. Matsukura, T. Dietl, and and H. Ohno, nat. phys. **6**, 22 (2010).
[16] H. Chou, C. Lin, J. Huang, and H. Hsu, Phys. Rev. B **77**(24), 245210 (2008).
[17] E. Senthil kumar, S. Venkatesh, and M. S. Ramachandra Rao, Appl. Phys. Lett. **96**(23), 232504 (2010).
[18] A. Ney, T. Kammermeier, V. Ney, K. Ollefs, and S. Ye, J. Magn. Magn. Mater. **320**(23), 3341 (2008).
[19] W. M. H. Oo, L. V. Saraf, M. H. Engelhard, V. Shutthanandan, L. Bergman, J. Huso, and M. D. McCluskey, J. Appl. Phys. **105**(1), 013715 (2009).
[20] K. Thakur, S. Gautam, K. H. Chae, M. Subramanian, R. Jayavel, and K. Asokan, J. Kor. Phys. Soc. **55**(1), 177 (2009).
[21] P. Thakur, K. H. Chae, J. Y. Kim, M. Subramanian, R. Jayavel, and K. Asokan, Appl. Phys. Lett. **91**(16), 162503 (2007).
[22] L. Zhang, J.-Q. Wang, J. Li, S. Zhang, Z. Jiang, J. Zhou, J. Cheng, T. Hu, W. Yan, X. Wei, and Z. Wu, Chem. Mater. **24**(9), 1676–1681 (2012).
[23] K. R. Kittilstved, D. A. Schwartz, A. C. Tuan, S. M. Heald, S. A. Chambers, and D. R. Gamelin, Phys. Rev. Lett. **97**(3), 037203 (2006).
[24] J. H. Guo, A. Gupta, P. Sharma, K. V. Rao, M. A. Marcus, C. L. Dong, J. M. Guillen, S. M. Butorin, M. Mattesini, P. A. Glans, K. E. Smith, C. L. Chang, and R. Ahuja, J.Phys.: Condens. Matter **19**(17), 172202 (2007).
[25] J. Jin, G. S. Chang, Y. X. Zhou, X. Y. Zhang, D. W. Boukhvalov, E. Z. Kurmaev, and A. Moewes, Appl. Surf. Sci. **257**, 10748 (2011).
[26] C. Dong, C. Persson, L. Vayssieres, A. Augustsson, T. Schmitt, M. Mattesini, R. Ahuja, C. Chang, and J. H. Guo, Phys. Rev. B **70**(19), 195325 (2004).
[27] J. W. Chiou, J. C. Jan, H. M. Tsai, C. W. Bao, W. F. Pong, M. H. Tsai, I. H. Hong, R. Klauser, J. F. Lee, J. J. Wu, and S. C. Liu, Appl. Phys. Lett. **84**(18), 3462 (2004).
[28] B. Straumal, A. Mazilkin, S. Protasova, A. Myatiev, P. Straumal, G. Schütz, P. van Aken, E. Goering, and B. Baretzky, Phys. Rev. B **79**, 205206 (2009).
[29] B. B. Straumal, S. G. Protasova, A. A. Mazilkin, A. A. Myatiev, P. B. Straumal, G. Schütz, E. Goering, and B. Baretzky, J. Appl. Phys. **108**(7), 073923 (2010).
[30] A. L. Shluger, K. P. McKenna, P. V. Sushko, D. M. Ramo, and A. V. Kimmel, Modell. Simul. Mater. Sci. Eng. **17**(8), 084004 (2009).
[31] P. Liu and J. Tang, Journal of physics. Condensed matter : an Institute of Physics journal **25**, 125802 (2013).
[32] A. Chakrabarty and C. H. Patterson, Phys. Rev. B **84**, 054441 (2011).
[33] M. Berciu and R. N. Bhatt, Phys. Rev. Lett. **87**(10), 107203 (2001).
[34] A. Kaminski and S. Das Sarma, Phys. Rev. Lett. **88**, 247202 (2002).
[35] A. Kaminski and S. Das Sarma, Phys. Rev. B **68**, 235210 (2003).
[36] S. von Molnar and T. Kasuya, Proc. tenth Intl. Conf. Phys. Semicon. **233** (1970).
[37] B. Thole, G. van der Laan, J. Fuggle, G. Sawatzky, R. Karnatak, and J. M. Esteva, Physical Review B **32**(8), 5107–5118 (1985).
[38] H. Chou, C. P. Lin, H. S. Hsu, and S. J. Sun, Appl. Phys. Lett. **96**(9), 092503 (2010).
[39] P. Majumdar and P. Littlewood, Phys. Rev. Lett. **81**(6), 1314 (1998).
[40] K. Sato, T. Fukushima, and H. Katayama-Yoshida, Jpn. J. App. Phys. **46**(No. 28), L682–L684 (2007).
[41] R. Morgunov, A. Dmitriev, and O. Kazakova, Phys. Rev. B **80**, 085205 (2009).
[42] L. Ottaviano, A. Continenza, G. Profeta, G. Impellizzeri, A. Irrera, R. Gunnella, and O. Kazakova, Phys. Rev. B **83**, 134426 (2011).

[43] H. Tang, K. Prasad, R. Sanjinès, P. E. Schmid, and F. Lévy, J. Appl. Phys. **75**(4), 2042 (1994).
[44] J. H. Yao, H. H. Lin, and T. S. Chin, Appl. Phys. Lett. **92**(24), 242501 (2008).
[45] B. L. Altshuler and A. G. Aronov, *Electron-Electron Interactions in Disordered Systems* (North Holland, Amsterdam, 1985).
[46] N. F. Mott, Philos. Mag. A **19**, 835 (1969).
[47] R. Khosla and J. Fischer, Phys. Rev. B **2**(10), 4084 (1970).
[48] T. Dietl, J. Phys. Soc. Jpn. **77**(3), 031005 (2008).
[49] Q. Xu, L. Hartmann, H. Schmidt, H. Hochmuth, M. Lorenz, R. Schmidt-Grund, C. Sturm, D. Spemann, and M. Grundmann, Phys. Rev. B **73**, 205342 (2006).
[50] J. Jaroszyński, T. Andrearczyk, G. Karczewski, J. Wróbel, T. Wojtowicz, D. Popović, and T. Dietl, Phys. Rev. B **76**(4), 045322 (2007).
[51] T. Andrearczyk, J. Jaroszyński, G. Grabecki, T. Dietl, T. Fukumura, and M. Kawasaki, Phys. Rev. B **72**, 121309 (R) (2005).
[52] T. Dietl, T. Andrearczyk, A. Lipińska, M. Kiecana, M. Tay, and Y. Wu, Phys. Rev. B **76**, 155312 (2007).
[53] J. R. Neal, A. J. Behan, R. M. Ibrahim, H. J. Blythe, M. Ziese, A. M. Fox, and G. A. Gehring, Phys. Rev. Lett. **96**(19), 197208 (2006).
[54] X. H. Xu, H. J. Blythe, M. Ziese, A. J. Behan, J. R. Neal, A. Mokhtari, R. M. Ibrahim, A. M. Fox, and G. A. Gehring, New J. Phys. **8**, 135 (2006).
[55] P. A. Lee and T. V. Ramakrishnan, Rev. Mod. Phys. **57**(2), 287 (1985).
[56] J. M. D. Coey, M. Venkatesan, and C. B. Fitzerald, Nature Mater. **4**(2), 173 (2005).
[57] B. Pal and P. K. Giri, J. Appl. Phys. **108**(8), 084322 (2010).